Superalloys 2004
Edited by K.A. Green, T.M. Pollock, H. Harada,
T.E. Howson, R.C. Reed, J.J. Schirra, and S. Walston
TMS (The Minerals, Metals & Materials Society), 2004

EVALUATION OF THE IN 939 ALLOY FOR LARGE AIRCRAFT ENGINE STRUCTURES

Göran Sjöberg[1] , Dzevad Imamovic[1], Johannes Gabel[2], Oscar Caballero[3], Jeffery W Brooks[4], Jean- Pierre Ferté [5], Ariane Lugan[6]
[1]Volvo Aero Corporation, Trollhättan, Sweden
[2]MTU,Aero Engines, Munich, Germany
[3]ITP , Industria de Turbo Propulsores, Zamudio, spain
[4]QinetiQ Limited, Cody Technology Park, Farnborough, United Kingdom
[5]Snecma Moteurs, Evry, France
[6]TWI, Great Abington, Cambridge, United Kingdom

Keywords: IN 939, structures, casting, sprayforming, welding, over-aging, mechanical properties

Abstract

The airfoil alloy IN 939 has been evaluated for the use in large aircraft engine structures. Castability trials, including sprayforming, structural welding, with electron beam (EB) and with laser, as well as repair with TIG-welding have been performed. Brazing has also been evaluated while different heat treatment schedules for pre- and post-welding and for the solution and age cycle were reviewed. Mechanical property data, tensile, creep, LCF, FCG, were established for several temperatures on material excised from large castings and on weldments. The performance of the sprayformed (SF) material was superior to the conventionally cast (CC) material but notch-sensitivity was noticed in creep testing.

Introduction

The alloy IN939 was developed for turbine airfoils and has been used extensively in industrial gas turbines. However the development of the alloy and the joining technology required for application to large structural components in aero engines includes significant risks, which have been investigated within this study.

The alloy 718 has been the obvious and very successful choice for hot structures with complex geometry since large scale vacuum investment casting technology became available. The γ”- phase hardening 718 alloy has excellent weldability compared with other high-strength γ’- hardening superalloys, due to the low levels of Al and Ti [1]. The excellent weldability is also the main reason for the popularity, since it permits substantial repair work on large castings where this is practically inevitable.

However, alloy 718 finds only limited use above 650 °C due to the coarsening of the γ”- precipitation. Since a weldable precipitation hardening alloy without this temperature restriction is very attractive, numerous attempts have been made to improve the thermal stability of the γ”-phase [2] along with the development of new alloys (notably René 220, RS5 and lately Allvac 718+) but all efforts have achieved limited success.

As a consequence, attempts to use γ’- hardening alloys, with their inherent higher temperature capability, for complex structures [3] are easy to understand. IN 939 is a reasonable choice among such alloys since the chemistry balances the weldability with adequate strength [1] which makes it a likely candidate for such applications and, in this context, high purity (low N, O, S and P) IN 939 material is today available for reduced risk of cracking in the heat affected zone (HAZ) during welding [4].

Perhaps the best means to reduce the susceptibility to cracking during welding of this class of γ’-hardening superalloys is to overage the material initially. The potential of such a heat treatment was recognized early in comprehensive studies on René 41 [5] and later also specifically for IN 939 [6]. The lower yield stress and the improved ductility in the over-aged condition reduce the weld stresses and thus the risk for cracking, not only during the actual weld process, the HAZ – cracking, but also during a subsequent heating cycle when strain-age cracking can occurs.

Cast material

Several castings were produced in this development program, the chemistries of which are given in table I.

The ring-strut-ring structure model, O.D. 800 mm, shown in figure 1, represents a full size engine part used in our evaluation. A range of constraint features was incorporated including struts with different fillet radii, stiffener ribs at different locations, engine mounts and bosses. Although, only one investment casting was produced from a SLA pattern, it was very successful as a first casting, mainly due to earlier experience with casting this type of complex geometry application in IN 939, at Howmet, Le Creusot in France.

Table I. Actual Chemical composition in weight percent

	C	Cr	Co	Mo	W	Ta	Nb	Al	Ti	Zr	B	P	S	Ni
Structure Casting	0.15	22.4	19.0	<0.01	2.02	1.45	1.02	2.00	3.71	<0.003	0.004	<0.005	<0.001	Bal.
Ring casting	0.14	22.5	18.9	0.10	2.03	1.37	0.97	1.92	3.68	0.059	0.009	0.002	<0.002	Bal.
Sprayformed rings	0.14	22.3	18.9	0.03	2.04	1.46	1.0	1.92	3.74	0.092	0.009	0.002	0.0005	Bal.

Figure 1. CAD-model of the complex structure , O.D. 800 mm, with varied constraint features for the evaluation of the suitability of IN939 for this type of castings.

Intermediate size castings were also produced by investment casting for the evaluation of different types of welded joints and for generating mechanical property data for large grain size material as may be found in thicker sections of cast structures. Seven conventionally investment cast (CC) (O.D. 330, t. 25, h. 90 mm) were made by PCB, Precicast, Bilbao, Spain, figure 2 and three sprayformed (SF) rings (O.D. 380, t. 40, h. 180 mm) by STI, Michigan, USA. All rings were hot isotatically pressed (HIPed) after the gating systems had been removed by heating at 6 °C/min, holding 1160 °C (1079 °C for the SF material) /3h, at 1000 bar, cooling at 5 °C/min to 650 °C.

Figure 2. Conventionally cast (CC) rings, O.D. 380, used for structural welding trials and for the evaluation of mechanical property data.

Castability

The ability to fill thin sections was tested using various strut wall thickness and tapers, which were incorporated in the structural model, figure 1. A thin, 2 mm, front plate was incorporated for the same reason. However, no shrinkage was found in these areas of the structural casting, which indicates the high fluidity of the IN 939 alloy and its ability to fill thin sections.

Shrinkage was, however, found at other locations. One severe case (level 5 on the ASTM-192 reference chart) was found at the undercut of the outer ring where it met with the leading edge of a strut, with 3 mm wall thickness and 12 mm fillet radius. The weakness introduced by the shrinkage gave rise to cracking later, as shown in figure 3 a. In the software simulation of the casting process, this region was also indicated as a potential problem area as mass accumulates without proper feeding and this problem could thus have been solved by using a modified gating system.

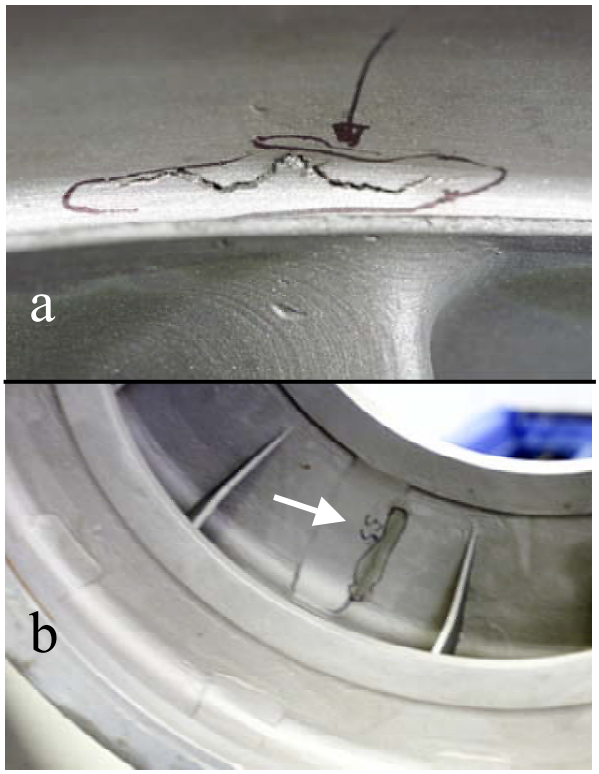

Figure 3. Cracks in demo-casting. a) Crack caused by shrinkage and geometrical constraint at a strut-ring intersection. b) A large crack at the thick-thin junction between a gate (here removed) and the thin front plate.

Large cracks were also found in the thin front plate at the gate contact areas, as shown in figure 3 b (he gating system has been removed here). In the as cast condition, only one crack of this type was found, but after HIP cracks were found at all six gate contact areas. The microstructure at these locations, examined by a replica, is seen in figure 4 a. The interdendritic areas are heavily decorated with eutectic MC-carbides formed during slow solidification, most likely due to the large thermal mass of the internally located gates. Since the MC-carbides do not go into solution below the solidus temperature of the alloy [7], the brittleness introduced by this carbide morphology will remain

during subsequent heat treatments. Weld repair in this type of brittle microstructure, with the added risk of constitutional liquation due to the presence of the carbide eutectic, is not advisable. Only adjustments of the gating system may solve this problem.

The constraint imposed by the stiff gating system is certainly a factor which contributed to the first crack produced during the casting process, which becomes obvious when the microstructure of the etched surface in this area, as shown in figure 4 b, is interpreted. The cast material is here, locally, partly recrystallized, not least evident from the presence of twins and such recrystallization could hardly take place without substantial plastic deformation having taken place during the casting process. This problem also has to be addressed by modification of the gating system.

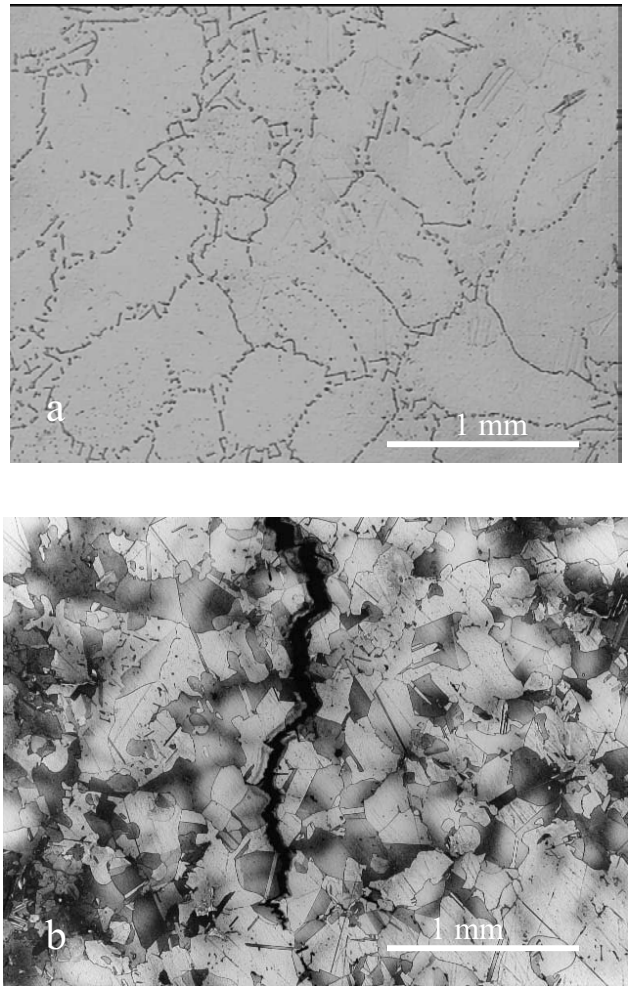

Figure 4. a) Replica of the as polished material after HIP, close to the crack at the gating contact area, showing MC-carbid eutectic in interdendritic areas. b) The etched microstructure of the partly recrystallized material surrounding the vertical crack, reveals localized deformation.

Heat treatment

Since different means of joining and repair by welding are integral and important parts of our evaluation the choice of pre- and post-weld heat treatments was important together with a review of the very long solution and age heat treatment cycle, developed for optimal mechanical properties in airfoil applications.

Pre-weld heat treatment – overaging

Overaging involves the solution of all γ' at high temperatures and a re-precipitation, also at high temperature , to produce as large γ' as feasible to make the material as soft as possible.

The temperature 1160°C is the standard solution temperature, not only for the solution of γ' but also for other phases and, with a dwell time of at least 4 hours, all carbides, except for the MC-type, as well as most of the η – phase will go into solution [6]. During slow cooling, in the interval between 1100 °C and 1000 °C, the η – phase precipitates which may embrittle the structure [8]. However, in IN 939 the η – phase morphology is plate-like, which is considered to be less detrimental to ductility than the cellular morphology [9] found in other superalloys. Overaging experiments carried out by Shaw [6] supports this and elongations of up to 13 % were measured after dwell times of 20 hours at 1052 °C.

An additional benefit from the slow cooling is the development of serrated grain boundaries, a morphology which improves stress-rupture life, ductility and resistance to strain-age cracking [10]. In our evaluation, the cooling rate of 1 °C /min, from 1160 °C to 760 °C followed by air cool, was considered appropriate. The hardness obtained was 356 HV compared with 430 HV in the alloy in the fully heat-treated condition. In the solution state, the hardness, as measured on thin test specimens water quenched from 1160 °C, was 369 HV.

With the chosen overage heat treatment, some η – phase precipitates, but this may, as indicated above, be accepted. In order to closer examine the η – phase behavior during significant deformation a simple bend test was performed. A 4 mm thick test sample, in the overaged state, was bent by hand at room temperature until partial fracture occurred. At the severely deformed material in front of the crack tip, it was found that the η – phase platelets adhere well to the matrix and also that they deform plastically. In contrast, as seen in figure 5, the MC carbides, in the same strain field, readily separate from the matrix and also break up.

Post-weld heat treatment – heating to the solution temperature

The strain-age cracking problem is a rather complex phenomenon involving precipitation not only of γ' but also of carbides in highly strained heat affected zones (HAZ) at intermediate temperatures during the heating up cycle after welding [11]. As mentioned before, early work on René 41 [5] made comprehensive attempts to monitor this problem through careful characterization and the definition of time temperature crack diagrams. From such diagrams it is evident that it is mandatory to stay as short a time as possible at intermediate temperatures, where the γ'-precipitation rate is highest, in order to minimize the problem. To reduce the thermal stresses,

produced by rapid heating in large parts with complex geometries and high constraint factors, it is also advisable to

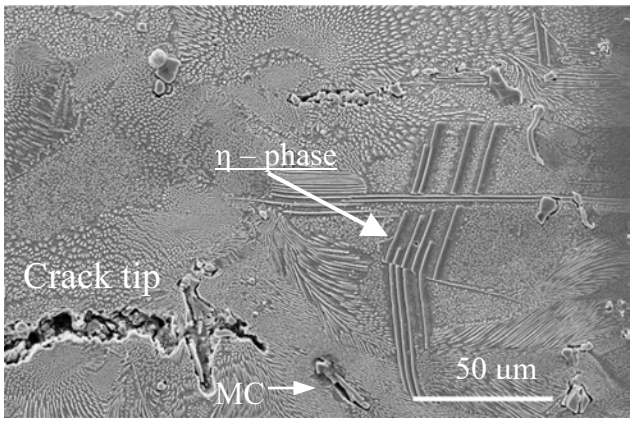

Figure 5. A crack tip, to the lower left, in a partly broken overaged specimen of CC-material with η – phase platelets to the middle right. The strong adherence of the η – phase to matrix in the heavily deformed material in front of the crack is evident as well as its ability to deform.

slowly heat the part to a temperature below the critical temperature interval to level out the thermal gradients, followed by heating as fast as possible through the critical range. The heating rate must, however, be limited since unacceptable levels of new thermal stresses may develop. Clearly, part geometry and furnace conditions are also important parameters.

The following post-weld heating cycle was chosen.

R.T – 565 °C / 9 – 13 °C/min.; 565 °C – 1037 °C / 20 – 24 °C/min.; 1037 °C – 1160 °C / 4 – 8 °C/ min.

Solution and Aging

The ageing cycle for IN 939, as originally developed for optimal properties in airfoil applications, was in four steps and emphasized creep [12]. For hot aircraft engine structures, however, although creep is one of the design criteria, good fatigue properties, especially in the low cycle regime, are of prime importance, due to the fact that it is only during take-off that the highest stress and temperatures levels are reached and that it is mainly this part of the total service time that governs the life of a component. Yield strength and ductility may consequently serve as first guidelines for the choice of a suitable heat treatment rather than the creep properties. Since the four step heat treatment, as mentioned, is also very time consuming (50 hours at temperature, plus heating and cooling time) alternative heat treatments with shorter duration have been considered [7 , 6].

The following solution-aging cycle was chosen for our evaluation – all steps performed in a protective atmosphere.

Step 1: (heating up as per the post-weld cycle above); 1160 °C, 4 hr.; cooling 3 – 7 °C/min; 900 °C – R.T.; fast gas cooling.

Step 2: 1000 °C, 6 hr; fast gas cooling (15 – 20 °C/min)

Step 3: 800 °C, 4 hr; gas cooling (5 – 10 °C/min)

The slow cooling rate from 1160 °C down to 900 °C is, as already mentioned, beneficial to the mechanical properties due to the serrated grain boundaries formed, a feature which reduces the tendency for oxidation assisted intergranular high temperature creep crack growth in both γ' [13] and γ" [14] forming superalloys.

The serrations, or rather undulations, of the grain boundaries are obvious from the micrographs in figure 6. The coarse grain size (1 – 3 mm) and the dendritic pattern of the cast material are also revealed by the Kallings etch. As may be noticed, the undulations relates to the pattern of the dendrites. MC-carbides are concentrated into the interdendritic areas due to the local enrichment of Ti, Nb and Ta [7]. The large MC-carbides, seen at the higher magnification in figure 7, decorate the grain boundary and may contribute to the stability of this morphology during the two solution heat treatments of the casting.

Figure 6. Microstructure of the CC IN 939 in the fully heat treated condition. Kallings etch.

In figure 7, the grain boundary morphology on a much finer scale is seen with decorations of $M_{23}C_6$ carbides in addition to the large MC carbides. While generally considered as important for creep properties, $M_{23}C_6$ carbides, which precipitate at rather low temperatures, may not primarily be responsible for the evolution of the serrated structure. It has been suggested that this structure is developed by the primary γ'- precipitation during slow cooling above the solvus temperature [10, 15] of the $M_{23}C_6$ carbides (approximately 1000 °C). However, slow cooling below this temperature is also important in order to avoid

continuous carbide films, which seriously reduce ductility [6, 10, 7].

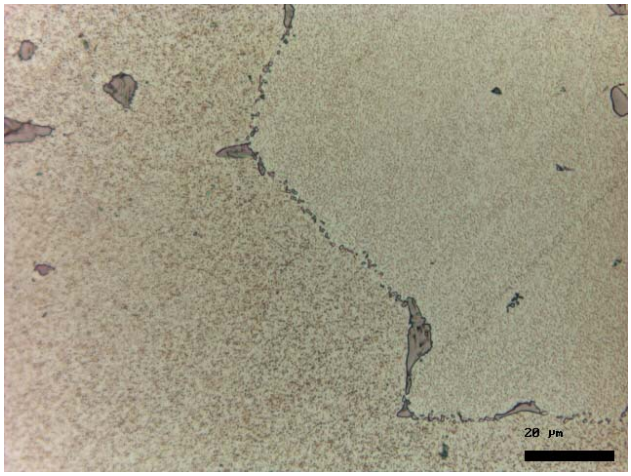

Figure 7. Serrated grain boundary microstructure of the CC IN 939 in the fully heat treated condition. Kallings etch.

For the SF-material the solution temperature had to be limited to 1093 °C in order to avoid grain growth. Compared with the CC-material the SF – material consists of very fine grains, as is evident in figure 8.

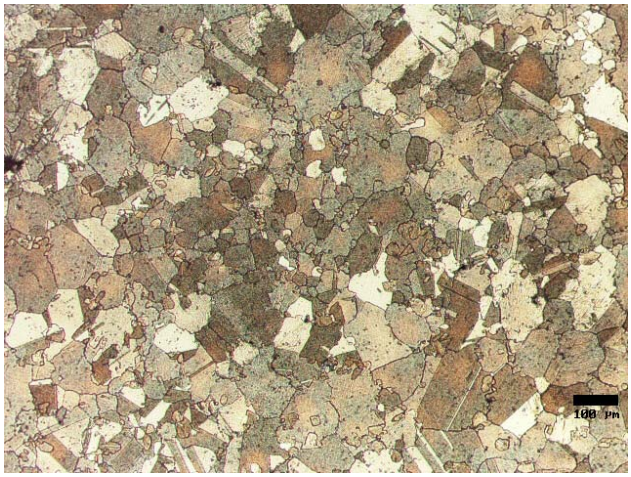

Figure 8. Fine grain microstructure of sprayformed material.

Weldability

Structural welding was performed with electron beam (EB), and with laser welding, both with and without C263 filler material.The EB welding was done at ITP, Bilbao in Spain, in a 150 kV x 100 mA, FERRANTI – VXHV 2 equipment. Laser welding without filler material, under the responsibility of Snecma Moteurs, France, was carried out at TWI in the UK on a 4kW, CW, HL 4006D, flash-lamp-pumped, Nd:YAG laser. MTU was responsible for the laser welding with filler material which was subcontracted to EADS and made with a HL3005D-I beam source.

After overaging, each casting was split into 5 concentric rings by electro-discharge wire machining (EDWM). The oxidized surface, left by the EDWM-process, was removed and the ring thickness reduced to 3 mm by a turning operation. To economize with the test material the machined rings were at the same time split into different, appropriate, heights as illustrated in figure 9.

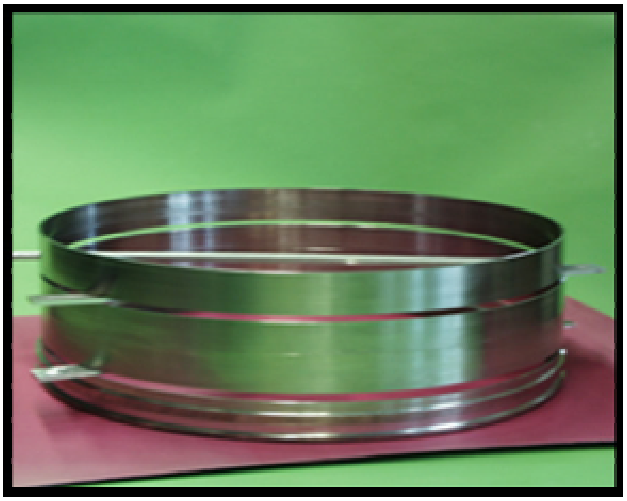

Figure 9. Rings excised from castings by electro-discharge wire machining to 4 mm thickness, cleaned by turning to 3 mm and split into different heights to accommodate for the structural welding set-ups.

ITP and MTU introduced a small centering lip for perfect alignment of the joint. For the laser welding without filler material a butt weld joint was evaluated at TWI.

Numerous weld bead trials were performed with various parameter settings to obtain the best results for each welding method with respect to weld geometry and internal defects, HAZ-cracking and fused zone porosity. X-ray, FPI as well as extensive metallographic cross-sectioning were used for the evaluation. In all, the results from the welding trials were much better than anticipated.

Very few cracks were found, mainly confind to the start and stop overlapping sections, and strain age cracking was virtually absent. Contrary to the SF material, the EB-welding of the CC material produced some internal HAZ micro-cracks. The largest crack detected was 0.5 mm and from a practical point of view this quality level is quite acceptable since this size is well below NDT levels of detection.

The high porosity in some laser welds with filler material, figure 10, was considered as a major problem with the welding parameters having a strong influence. It is evident that the frequency of small pores is higher in the SF-material than in the

CC-material. The maximum pore size is, though, smaller in the SF-material. In general, the amount of porosity was higher in the laser welds where filler material was used, as seen for the SF-material by comparing the cross-section in figure 10 with the corresponding in figure 11.

Figure 10. Longitudinal sections, as polished, through laser welds with C 263 filler material on sprayformed material (top) and CC-material (bottom). Sheet thickness is 3 mm.

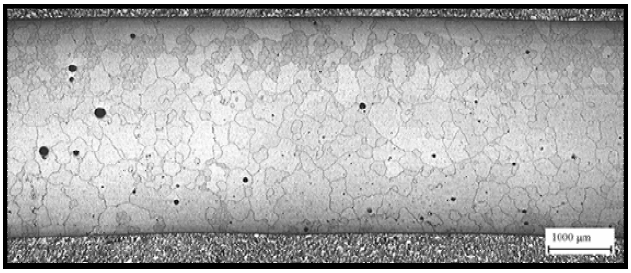

Figure 11. Longitudinal sections through laser welds without filler material on spray cast material, slightly etched. Sheet thickness is 3 mm.

In contrast, the EB-welds contained very few pores which may be due to the beneficial influence of the vacuum environment in the EB- welding chamber on the weld pool.

As mentioned above, the porosity varied considerably with the chosen welding method and parameters; the amount being from 0 to 1 %, the maximum pore size from 0.2 to 1 mm. Laser welding without filler material was selected as the preferred method and, as such, was also used to produce the ring, in the CC-material, for the mechanical testing of a weld. A cross-section of the weld joint made by the optimized process is shown in figure 12. Very few pores were detected and the maximum size was less than 0.2 mm.

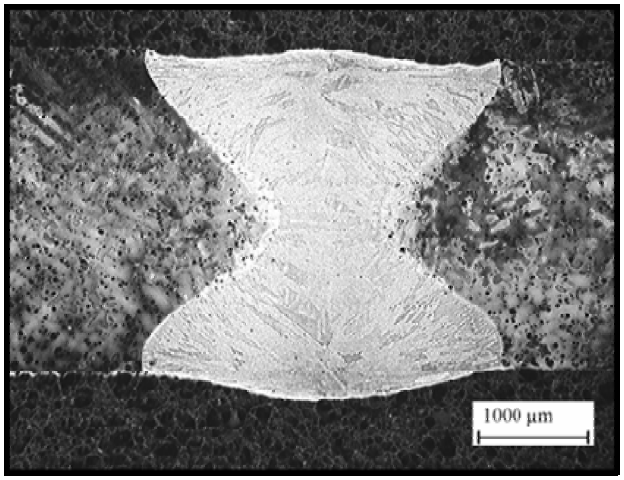

Figure 12. Cross-section of the optimized laser weld without filler material in CC-material. Before PWHT, Kallings etch.

Repair by welding and brazing

Large structures with complex geometry cannot realistically be produced by casting without substantial repair work. A consistent evaluation of the 'repairability' of IN 939 must, by nature, be very comprehensive and far from the scope of this work, which was simply to show that it is possible to grind out defects and build back geometry by welding in the overaged material, with C263 as filler metal, in heavily constrained areas. The success of such a grind out and welding procedure is shown in figures 13 and 14, respectively. Repairs with lower alloy content material, like C263, have considerably lower strength than the cast material and can, therefore, only be accepted in low stress areas or where the surrounding material can carry the extra load. To our knowledge, IN 939 weld wire is not available commercially.

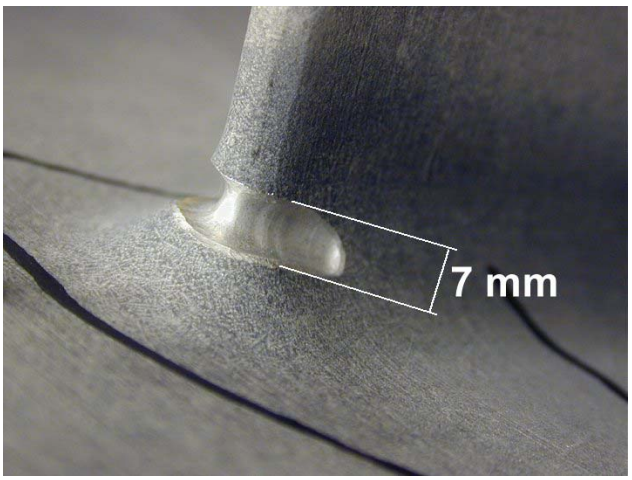

Figure 13. Grind out in heavily constrained area prior to repair welding.

Figure 14. Successful weld repair with C263 filler material of the grind out in figure 13.

Brazing experiments were made with alloy mixtures of D15 and René 80 at temperatures close to the solution temperature of IN 939 to evaluate compatibility. Other criteria were hot strength, oxidation resistance, gap filling, wettability and flow behaviour

It was found that restoration of worn surfaces using a mixture of 60% D15, 40% René 80 is promising. The repair of was not successful regarding as tensile strength of the joints was only about one fifth of the base material.

Mechanical testing

As summarized in table II, various mechanical properties were determined for the CC-material as well as for the SF-material in the fully heat treated conditions and also for structural welds. Within the scope of this paper it is only possible to discuss selected properties.

Tensile properties

As shown in figure 15, the yield strength of the SF material is in the order of 10 % higher than that of the CC material up to 700 °C, a difference that is reduced to around 5 % at 800 °C. The yield strength of the welded material is slightly lower than of the CC material at temperatures up to 700 °C.

The ultimate tensile strength, figure 16, of the SF is considerably higher, around 20 %, than of the CC material which results from larger strain hardening of the SF material due to the better ductility.

Table II. Mechanical test plan

Conventionally cast Material	
Test	**Test condition**
Tensile	RT, 500, 600, 700, 800 °C
LCF	650 °C, R = 0, smooth
Creep rupture	700 and 800°C
LCF	650 °C, R = -1, notched KT=2.2
LCF	650 °C, R = 0, notched KT=2.2
FCGR	RT and 650 C, duplicates
Notched stress rupture	650 °C, 689 MPa per ASTM E292
Welded Material	
Test	**Test condition**
Tensile	RT ,500,600,700,800 °C
Creep rupture	700 and 800°C
Hardness	RT
LCF	650 °C, R = 0, smooth
Sprayformed Material	
Test	**Test condition**
Tensile	RT , 500, 600, 700, 800 °C
Creep rupture	700 and 800 °C
LCF	650 °C, R = -1, notched KT = 2.2
LCF	650 °C, R = 0, notched KT = 2.2
LCF	650 °C, R = 0, smooth
FCGR	RT and 650 C, duplicates, R = 0.05
Notched stress rupture	650 °C, 689 MPa per ASTM E292

It may seem surprising that the test specimens of the CC-material with welds are stronger than specimens from the same material without welds. However, the rational here is that the material subjected to welding has received an extra high temperature solution heat treatment as an integral part of the pre-weld over-age heat treatment with improved homogeneity and increased strain hardening as a result.

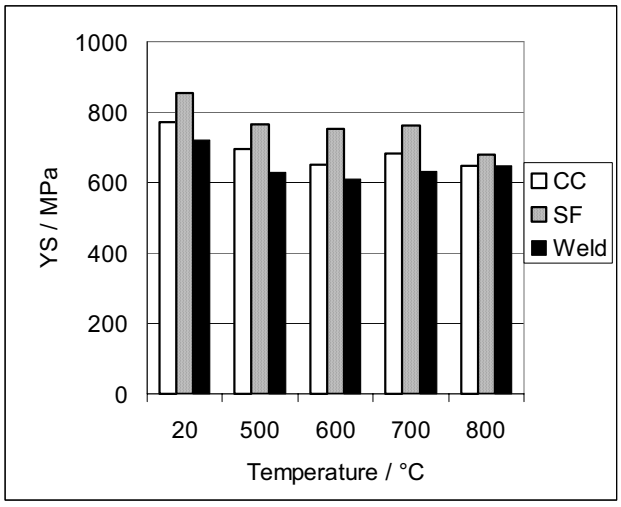

Figure 15. Average yield strength at various temperatures

That the actual welds (without filler material) are stronger than the matrix material may easily be understood in terms of the finer cast structure in the actual weld bead material.

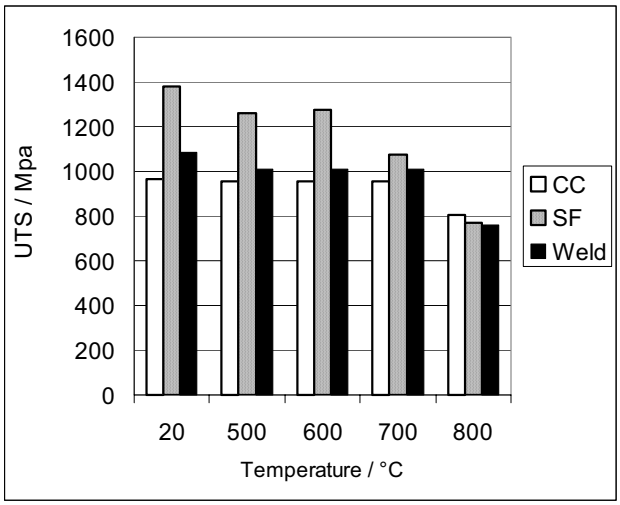

Figure 16. Average ultimate tensile strength at various temperatures

Creep and stress rupture properties

The creep properties are summarized in figure 17. As may have been anticipated, the CC-material benefits from the larger grain size in comparison with the SF-material and, for the same reason, was also comparable with the welded material. These values compare well with those reported for similar temperatures but with a four stage heat treatment [7].

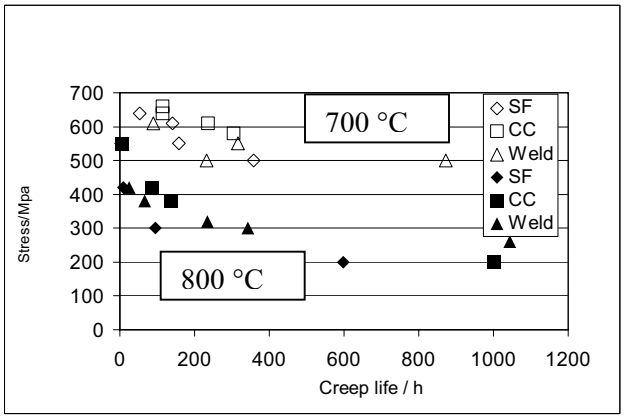

Figure 17. Creep properties.

Combined, smooth and notched, stress rupture testing was performed at 650 °C on CC- and SF- material at a stress level of 689 Mpa with two test bars of each. Here both SF test bars failed in the notch (0.13 mm radius) and sustained the load under approximately only one third of time , 181 and 185 hrs versus 1129 and 567 hrs for CC test bars which failed in the smooth section. The mechanisms involved in the notch sensitivity of superalloys [16] may be disputed but a strain/stress assisted grain boundary oxidation mechanism is part of the phenomena and the morphology of grain boundary precipitates is also important [14]. Therefore the fine grain size of the sprayformed material and the lack of grain boundary precipitation may also be important factors in the different behaviour of the CC and SF materials. Stress rupture notch sensitivity is also related to hold time crack growth and for IN 939 it has been shown that the crack growth rate can be reduced if grain boundary morphology and chemistry are properly controlled [3].

Fatigue properties

The low cycle fatigue properties for SF- and CC-material at 650 °C are summarized in figure 18. A few test samples of the CC-material, not included in the graph, fractured during the first load cycle, due to the coarse grains and unfavourable orientation in the test samples.

The fatigue life of the SF-material is evidently a factor of hundred better than the CC-material due to the higher strength and ductility of the refined IN 939 material.

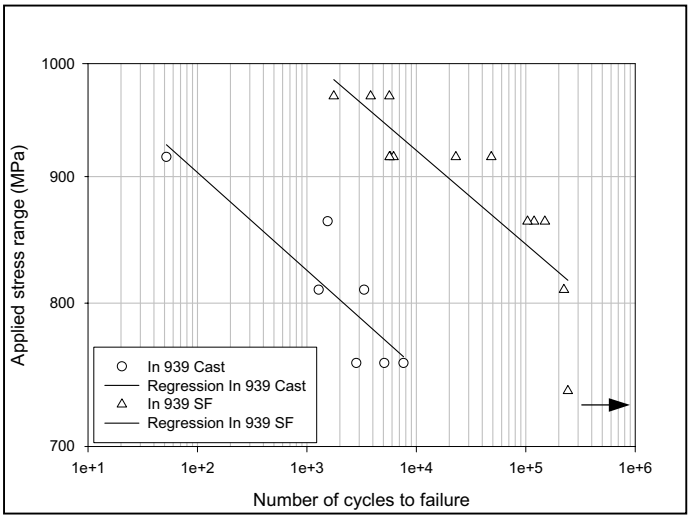

Figure 18. Low cycle fatigue properties of CC – and SF-material at 650 °C, R = 0, frequency 0.25 Hz and trapezoidal 1-1-1-1 wave form.

Fatigue crack growth (FCG) was measured on both SF- and CC-materials at room temperature and at 650 °C. As may be seen in the plot of data points, in figure 19, from the testing of the CC-material at 650 °C the scatter and irregularities are considerable larger when compared with the SF-material in figure 20. Again this may be attributed to the large grain size of the CC-material and the orientations of the grains.

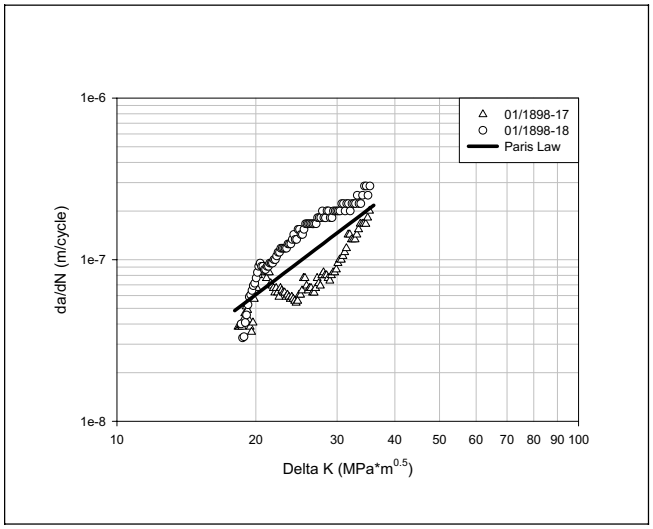

Figure 19. Fatigue crack growth (FCG) at 650 °C of the CC-material, R = 0.05, frequency 10 Hz and sinusoidal wave form.

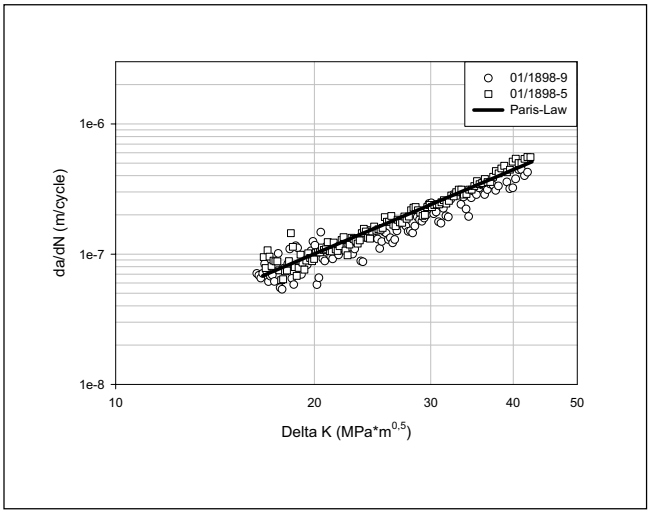

Figure 20. Fatigue crack growth (FCG) at 650 °C of the SF-material, R = 0.05, frequency 10 Hz and sinusoidal wave form.

Still, it may be concluded that the FCG-rate of the SF - material is slightly higher than of the CC - material, especially at the higher stress intensities. This agrees with the opinion that large grain sizes are good for crack growth resistance. As indicated earlier, the variation in crack growth may be much higher for long hold times due to the documented difference in notch sensitivity of the SF - material at this temperature.

Conclusions

1. Large complex aircraft engine structures may be cast as one-piece castings in alloy IN 939.

2. Moderate size TIG-repair welds can successfully be made in overaged material with soft filler material as C263.

3. Acceptable structural welds can be made with EB- and laser welding with and without C263 filler material

4. A short duration two stage solution and age heat treatment may be used with adequate properties for structures

5. Sprayformed material has superior low cycle fatigue properties compared with conventionally cast IN 939.

6. Short cycle fatigue crack growth rates are slightly higher in sprayformed material compared with conventionally cast material.

7. Sprayformed material suffers from notch-sensitivity at 650 °C.

1 M. Prager and C.S. Shira. “Weldability of Gamma-Prime Strengthened Alloys” (Welding Research Counsel Bulletine, no. 129, 1968).

2 Edward A. Loria. “Rene220: In Retrospect and Prospect”, *Superalloys 718, 625, 706 and Various Derivatives*, ed. E.A. Loria (TMS, 1994), 739 - 750.

3 Robert W. Hatala and John J. Schirra. “Developement of a Damage Tolerant Heat Treatment for Cast + HIP Incoloy 939”, *Superalloys 1996*, ed. R.D Kissinger et al. (TMS, 1996), 137 – 143.

4 “CM 939 Weldable™ Alloy” (CANNON-MUSKEGON CorporationTechnical Bulletin, August 2002).

5 T.F. Berry and W.P. Hughes, “A Study of Strain-Age Cracking Caracteristics in Welded René 41 – Phase II”, *Welding Research Supplement*,(nov. 1969), 505 – 513.

6 S.W.K Shaw, “Response of IN-939 to Process Variations”, *Superalloys 1980*, ed. John K. Tien et al., (Metals Park, OH: American Society for Metals, 1980), 275-284.

7 T.B. Gibbons and R. Stickler, “IN 939: Metallurgy, Properties and Performance, *High Temperature Alloys for*

*Gas Turbines,*eds. R. Brunetaud et al. (D. Reidel Publ. Comp., 1982), 369 – 393.

8 G.K. Bouse. "Eta (η) and Platelet Phases in Investment Cast Superalloys", *Superalloys 1996*, ed. R.D Kissinger et al. (TMS, 1996), 163 – 172.

9 Raymond F. Decker and Chester T. Sims, "The Metallurgy of Nickel-Base Alloys" *The Superalloys*, eds.C.T. Sims and W.T. Hagel (John Wiley & Sons, 1972), 1225 – 127.

10 R. Tamburaj et el., "Post-Weld Heat treatment Cracking in Superalloys", *International Metals Review*, 28 (2) (1983), 1 – 22.

11 W. Yeniscavich, "Joining", *The Superalloys*, eds.C.T. Sims and W.T. Hagel (John Wiley & Sons, 1972), 527 – 531.

12 K.M. Delargy et al., "Effects of Heatr Treatment on Mechanical Properties of High-Chromium Nickel-Base IN 939", *Materials Science and Technology,* 2 (1968), 1031 – 1037.

13 H.L. Danflou et al., "Formation of Serrated Grain Boundaries and Their Effect on the Mechanical Properties in a P/M Nickel Base superalloy", *Superalloys 1992*, eds. S. D. Antolovich et al. (TMS, 1992), 63 -72.

14 G. Sjöberg et al., "Grain Boundary δ-phase Morphologies, Carbides and Notch Sensitivity of Cast Alloy 718", *Superalloys 718, 625 and Various Derivatives, ed. E.A. Loria* (TMS 1991), 603 – 620.

15 A.K. Koul and R. Tamburaj, "Serrated Grain Boundary Formation Potential of Ni-Based superalloys and its Implications", *Metallurgical Transactions*, 16a (1985), 17

16 C. C. Law and M. J. Blackburn, "Notch-Ruptur Behavior of a Nickel-Base Superalloy at Intermediate Temperatures", *Superallovs 1980,* ed. John K. Tien et al., (Metals Park, OH: American Society for Metals, 1980), 651 – 660.